34th Annual International Conference of the IEEE EMBS
San Diego, California USA, 28 August - 1 September, 2012

Free Space Optical Link for Biomedical Applications*

Mohammad Y Abualhoul, Pontus Svenmarker, Qin Wang,
Jan Y. Andersson, and Anders J Johansson, *Member, IEEE*

***Abstract*— Free space optics is an interesting alternative for telemetry with medical implants, due to the high data bandwidths available at optical frequencies. Especially implanted brain-computer interfaces gives rise to large data sets that needs to be transmitted transcutaneous. In this paper we show that it is possible to establish such a link at near-IR wavelengths using a modulated reflector in the implant, thus keeping the laser and the detector on the outside. In addition, we show that it will not only work on short, i.e. touch, distances but also at larger distances, in the range of a meter. We have used an electro absorption modulator to modulate the reflection of an external laser source back towards an external detector. The only part of this system that needs to be implanted is the modulator and drive electronics. The study has been done both by Monte-Carlo simulations of a multi-layer model of a rat skull, and with an experiment demonstrating the feasibility of the link when transmitted through biological tissue. The results show that it is possible to establish a transcutaneous link with an external laser source and light detector, and an internal modulated reflector.**

I. Introduction

Free Space Optical communications (FSO) have attracted a lot of attention lately for a variety of applications in both medical and telecommunication fields [1]. The high speed, low cost, low power consumption, non-licensed and no limitation in bandwidth are some of the many reasons to deploy FSO in medical field, especially in such a short range applications where the weather attenuation has ignorable impact on the performance of FSO links.

The FSO links are usually designed to serve in last mile applications [2], where wire-lines, Radio Frequency (RF) and FSO wireless, using two transceivers, are used to interconnect communication nodes. Some of these edge nodes may be situated in remote areas, operating in strict and unusual environments such as the medical measurements, where it is hard to place and integrate a transceiver node with a power supply under living tissues. In this case, the FSO links, based on semi-passive optical retro-modulation technique are an interesting alternative to the traditional RF or FSO transceiver implementations [3][4]. Retro-modulation is the transfer of information between an optical transceiver and a semi-passive modulator that reflects optical signals [5], shown in Fig 1 Case B where it is realized with a modulator and a retro-reflector. This concept is different from the typical FSO communication systems based on two transceivers, operating in full-duplex approach, Fig. 1, Case A, in which retro-modulator with its encoding circuitry and nominal power source can be the entire communications terminal at the data collection side. A remotely located laser in the link will interrogate the RRM, where the interrogation beam is passively reflected by the RRM back to the receiving terminal with data impressed on it, while the biasing signal is responsible for modulating the electro-absorber modulator (EAM).

We have investigated the possibility to use a retro-modulated link to communicate transcutaneous, with the aim of using it to communicate with medical implants. This has the benefit of putting both the power consuming laser source and the detector on the outside of the human body, and thus conserving the energy of the battery in the medical implant. We have investigated this scheme both by simulations and by lab experiments where we have established a free space link over 1.5 meter with the light path going through a biological skin sample.

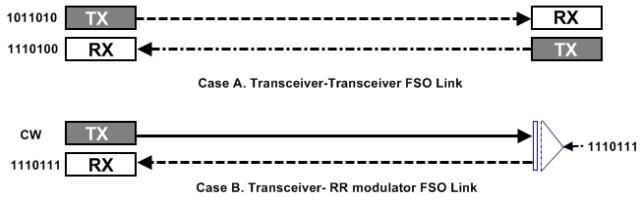

Fig.1: Case A, Transceiver-Transceiver FSO Link and Case B, Transceiver-Retro-Reflector Modulator Link.

II. Monte-Carlo Multi-Layered (MCML) Model

A. Overview

The Monte-Carlo for Multi-Layered (MCML) code [6] can simulate a multilayered model for a steady state light propagation in biological tissues. The approach assumes an infinitely wide layered structure and models an incident beam at a 90 degree angle to the surface. The beam radius, power level and beam profile are modeled independently by

*Research supported by a Linnaeus Grant from the Swedish Research Council (no. 60012701), a grant from the Knut and Alice Wallenberg Foundation (no. 2004.0119) and the Medical Faculty at Lund University. Biological tissue sample used under ethical permit M298-10

M. A. Abualhoul was with Lund University, Lund, Sweden.

P. Svenmarker is with Department of Physics, Lund University, Lund, Sweden.

Q. Wang is with the Department of Nanophysics, Acreo AB, 164 40 Stockholm, Sweden.

J. Y. Andersson is with the Department of Nanophysics, Acreo AB, 164 40 Stockholm, Sweden.

A. J. Johansson is with Department of Electrical and Information Technology, Lund University, Lund, Sweden. ajn@eit.lth.se

using convolution code [7] in order to convolute the fluence distribution, obtained from the MCML program. Four of the main six physical phenomena, absorption, scattering, reflectance and transmittance, are traced in MCML simulation to track the behavior of the penetrating photons. The behavior of the photons in the biological tissue are saved in a two dimensional array representing the normalized to the total number of photon packets, probability density of absorption, scattering, reflecting and transmitting as a function of depth (Z) and radius (R).

A. *Mouse Head Model*

The implemented model in MCML shown in Fig 2 consists of four types of tissues: scalp, skull, cerebrospinal fluid (CSF), grey matter and white matter respectively. The optical properties of each modeled layer, shown in Table 1, are extrapolated from the optical proparities of human brain tissues for the near infrared range [8]. Different layers of skull and CSF were used to model anatomical features, such as the varying density of the skull at different depths.

TABLE 1: OPTICAL PROPERTIES OF THE RAT SKIN MODEL

	μ_a (cm)$^{-1}$	μ_s (cm)-1	Refractive index (n)	Thickness (mm)
Scalp	0.40	200	1.4	0.12
Skull1	0.20	180	1.4	0.08
Skull2	0.10	150	1.4	0.23
Skull3	0.20	180	1.4	0.06
CSF1	0.03	0.01	1.0	0.06
CSF2	0.03	0.01	1.8	0.06
GM	0.25	250	1.4	3.00
WM	0.05	600	1.4	3.00

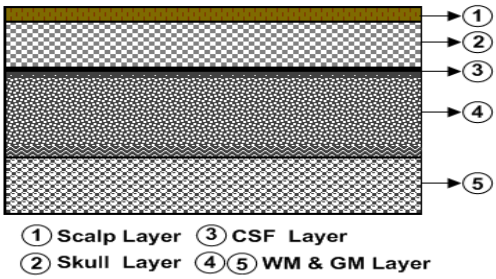

Fig.2. Monte-Carlo multilayer simulation model with the order and approximate relative thickness of the different layers: scalp, skull, cerebrospinal fluid (CSF), white matter (WM), grey matter (GM)

III. SIMULATION RESULTS

Monte-Carlo simulations were performed to validate the possibility of establishing a FSO link to an implanted modulated reflector, and to investigate how deep in the skull it would be reasonable to place it.

A. *Background Estimation*

We estimate the background level of photons reflected from the tissue itself by simulating the layers of tissue without any modulator present. The modulator was then added at different positions and the added reflection, i.e. changes in diffusion reflectance Diff_refl, was taken as the possible modulated signal.

Table 2 is representing a sample of the simulation results, where (No-Reflector) case stands for the simulation in which the last layer is defined to have a very high absorption coefficient in order to count the total number of photons. The background was 68% of the penetrated signal power. This background will be seen as a DC offset in the detector of the system. The same procedure was repeated for different locations of the Retro-Reflector layer, beneath different layers.

TABLE 2: MCML SIMULAION RESULTS FOR 4 CASES OF REFLECTOR PLACEMENTS, BENEATH RESPECTIVE LAYER.

	No-Reflector	**GM**	**CSF**	**Scalp**
diff_refl	0.6801	0.6814	0.8938	0.9337

B. *Reflector's Position and Dimensions*

The dimension of the reflective modulator will limit the placement, as larger depths in the tissue will require larger modulators. The anatomy of the intended user will constrain the maximum size possible to use in any one case.

We used the fluency data from the previous simulations to estimate the influence of the size of the reflector on the received signal. In this estimation a fluence threshold of 75% was used to find the minimum area needed. The simulation was repeated for the four different placements of the reflector. Fig. 3 gives the resulting area for all four placements.

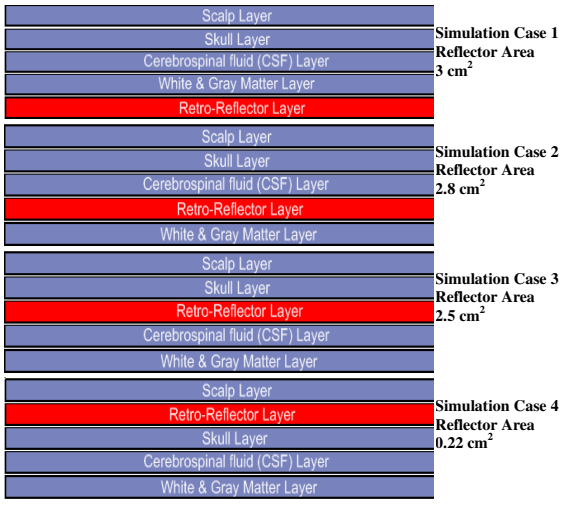

Fig. 3. Simulation steps and reflector different sizes for different depths

From these results we drew the conclusion that the only realistic placement in a rat or mouse was beneath the scalp, as these animals have skull sizes that cannot accommodate the needed reflector area for the other placements. For other animals, including humans, a placement beneath the skull could be feasible from this perspective.

IV. Experimental Setup

As the simulations showed that it would be possible to establish a link through tissue, we did a proof of concept experiment. The experiment was made on an optical bench, and a continuous wave laser Diode NT53-760 with collimated output wavelength of 854.52 nm and 2.9 mw output power was used as the source. The modulator was an electro absorption modulator (EAM) described in [9], and mounted next to the laser. A line of sight between the laser source and the EAM is achieved by aligning the transmitter terminal with the EAM and also between the EAM and the detector.

The experiment was setup to get a direct, perpendicular and focused beam at the center point of the 4 cm^2 skin sample. The beam radius at the sample was kept at 1 mm. The skin sample was taken from the back side of a ten months old laboratory rat. Measurements were made on fresh skin samples.

The EAM had 4 pixels, an $1.4 cm^2$ active aperture and maximum modulation depth response at 854.4 nm. It was modulated by a sinusoidal signal with an amplitude of 12 V. The distance separation between the laser/detector and the EAM was varied between 0.25 and 2.5 m with a step size of 0.25 m. A large area Si PIN photodiode S3548 with a 2.8 cm^2 active area was used as the detector together with a 10 cm diameter collecting lens. The transimpedance amplifier connected to the detector was able to support modulation speeds up to 5 kHz.

A. *Experimental results*

This experiment aims to present and compare the results from the measurements of the optical power and noise for the FSO link before and after inserting the skin sample in the beam path. Measurements and calculations of the atmospheric, geometric and modulator losses are given in Table 4.

TABLE 4: OPTICAL POWER LOSSES

Atmospheric Loss	Geometric Loss	Scattering Losses	Modulator Loss
0.036 dB	≥ 1 dB	(16 – 36) dB	1.6 dB

The experiment was conducted in a dark laboratory environment.

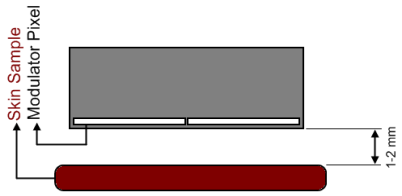

Fig. 4. The distance between the skin sample and the optical modulator surface

The skin sample was mounted in front of the modulator as shown in Fig. 4. The loss due to the scattering was calculated using equation 2,

$$P = \frac{A_{Lens}}{A_{Sph}} \approx \frac{r^2}{2R^2} \qquad (2)$$

where P is the probability for the scattered photons from the skin sample to hit the receiver lens, A_{Lens} and A_{Sph} are the area of the detection lens and the hemispherical area respectively and denoted by the hemisphere radius R and the lens radius r. Most reflected photons will be scattered in the tissue and lost.

The result gives that no more than 0.05 % of the modulated photons will hit the detector in the case of a 1.5 meter optical link. This equals a loss of 32 dB.

Fig. 5 show results of the detected modulated optical beam, obtained before and after inserting the skin sample, for a 0.5 m link length.

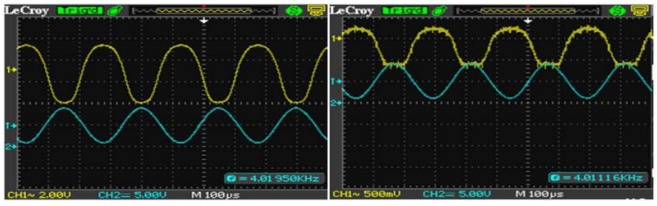

Fig. 5 Detected modulated optical beam before (Left) and after (Right) presenting the phantom, for a 0.5 meter link length. Input signal to the modulator is blue, received signal from photo detector is yellow.

B. *Optical Signal to Noise Ratio (OSNR) Measurements*

The OSNR investigation and the measurements were carried out for the FSO link as two types of measurements; the first investigation is without using the rat skin sample (FSO case), while the second investigate the influence after mounting the modulator aperture by the skin sample (SBO case). The analysis was done in the frequency domain of the detector signal by FFT.

The criteria for measuring the OSNR and the calibrations have been performed using a windows method. This method is defined to estimate the extracted power spectrum of the detected optical signal, representing the modulated signal and the optical noise in order to find the ratio between the both. The OSNR obtained by calculating the total Optical-

Signal-Power (OSP), represented by the red shaded area in Fig 15, while the optical noise power (ONP) is the numerical subtraction between the OSP and the total defined normalized power spectrum, which contains the OSP and ONP as it is depicted in the blue shaded area in Fig 16.

The two windows were chosen to be around the modulation center frequency (4 kHz). Those windows are starting from the same point of 1.9 KHz on the spectrum, in which the first window (W_s) is centered at the desired modulation frequency (4 kHz) and has bandwidth equal to 6 KHz, and the second window (W_{sn}), is confining the both normalized OSP and ONP for a power spectrum bandwidth equal to 100 KHz.

The numerical integration of the area under the peak, confined by normalized optical W_s and W_{sn} windows are resulting in normalized numerical values representing the distribution of the OSP and the total sum of the normalized OSP and ONP. In order to find out the OSNR for the acquired data for different optical link lengths, the ratio between the OSP and the OSN is calculated by using Equation 3.

$$OSNR \approx 20 * \log\left(\frac{OSP*W_s}{OSP*W_{sn} - OSP*W_s}\right) \quad (3)$$

Where OSP representing the Optical Signal Power and W_s and W_{sn} representing the optical signal window and the total optical power and noise window respectively.

TABLE 4: OSNR FOR DIFFERENT OPTICAL LENGTHS

Distance (m)	0.25	0.5	0.75	1.00	1.25	1.50	1.75	2.00
OSNR FSO (dB)	3.0	2.6	1.46	1.0	0.73	0.17	-1.2	-6.3
OSNR SBO (dB)	5.9	5.2	5.8	5.7	5.7	5.8	5.2	5.8

The calculated results of the OSNR measurements for the both FSO and SBO cases are shown in Fig. 6 and table 5.

The OSNR for FSO case starts at a maximum value of 3 dB at 0.25 m and trends downwards, increasing the distance to a minimum value of -6.3 dB at 2 meter, where it is almost constant over the optical link ranges in the SBO case (5.8 dB).

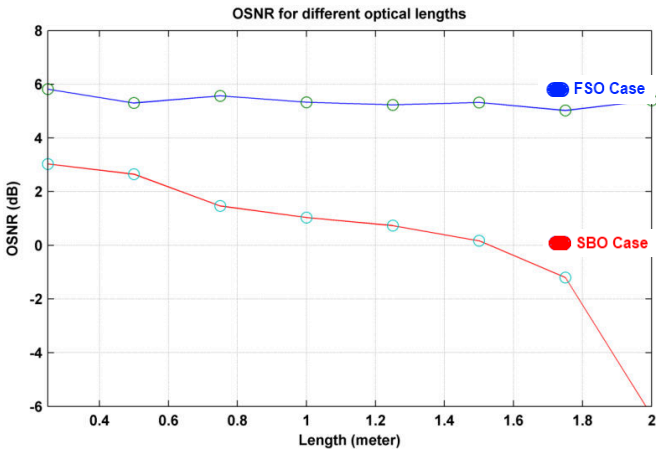

Fig.6 OSNR for different optical lengths

V. CONCLUSION

We have shown by simulations and experiments that it is possible to establish a FSO communication link in the IR region with a modulated reflector as the information transmitter over a distance of 1.5 m even when the light path to and from the modulated reflector is through biological tissue. This makes FSO an interesting candidate for communication with medical implants. This as the semi-passive nature of the modulated reflector makes it an attractive candidate for battery powered applications, as compared to modulated lasers or RF transmitters.

The drawback of the proposed link is the requirement of a direct line of sight. This will require a tracking system on the external unit, and an environment free from obstructions.

REFERENCES

[1] T. Plank, E. Leitgeb, and M. Loeschnigg, "Recent developments on free space optical links and wavelength analysis." 2011.

[2] Jayasri Akella, Murat Yuksel, and Shiv Kalyanaraman, "Multi-channel Communication in Free-Space Optical Networks for the Last-mile." 2009.

[3] M. Achour, "Free-space optical communication by retromodulation: concept, technologies, and challenges," 2004, vol. 5614, pp. 52-63. sept. 2004.

[4] National Research Laboratory, Modulating Retro Reflectors Laboratory, http://mrr.nrl.navy.mil/.

[5] Shay, T.M. et al., First Experimental Demonstration of Full-Duplex optical Communications on a Single Laser Beam, Proceedings of the 15th Annual AIAA/Utah State University Small Satellite Conference, 2001.

[6] L. Wang, S. L. Jacques, and L. Zheng, "MCML—Monte Carlo modeling of light transport in multi-layered tissues," Compute. Methods Programs Biomed. 472, 131–146 1995.

[7] L. Wang, S. L. Jacques, and L. Zheng, "CONV—convolution for responses to a finite diameter photon beam incident on multi-layered tissues," Compute. Methods Programs Biomed. 543, 141–150 1997.

[8] H. R. Eggert and V. Blazek, "Optical properties of human brain tissue, meninges, and brain tumors in the spectral range of 200 to 900 nm," Neurosurgery, vol. 21, no. 4, pp. 459-464, Oct. 1987.

[9] Q. Wang, S. Junique, D. Agren, B. Noharet, and J. Y. Andersson, "Fabry-perot Electroabsorption Modulators for High Speed Free-Space Optical Communication," IEEE Photonics Technology Letters, vol. 16, pp. 1471-1473, Jun. 2004.